

Full Research Paper

CdSe/ZnSe Quantum-Dot Semiconductor Optical Amplifiers

Muaffak A. Al-Mossawi¹, Ali Gehad Al-Shatravi² and Amin H. Al-Khursan^{1,*}

1 Nassiriya Nanotechnology Research Laboratory (NNRL), Science College, Thi-Qar University, Nassiriya, Iraq.

2 Physics Dept., Science College, Thi-Qar University, Nassiriya, Iraq.

* Author to whom correspondence should be addressed; E-Mail: ameen_2all@yahoo.com

Received: 04 January 2012 / in revised form: 28 February 2012 / Accepted: 09 April 2012 /

Published: 26 April 2012

Abstract: CdSe/ZnSe quantum dot semiconductor optical amplifier is studied theoretically where the core/shell structure is discussed. Absorption and emission coefficients and noise figure are studied. The emission coefficient obtained is higher than the similar structure of InGaAs/InP. A 25dB gain is obtained. A low noise figure (5.5dB) is obtained. A high output power can be obtained. The simulated structure can be used to develop photonic integrated circuits.

Keywords: CdSe/ZnSe; Linear absorption coefficient; Linear emission coefficient; Rate equations (REs); Noise figure.

1. Introduction:

Semiconductor quantum dots (QDs) are nanoparticles, structures with nanoscale dimensions, have unique properties arising from their small size and large surface-to-volume ratio [1]. They can be engineered to cover a wide emission wavelength either by cladding with higher bandgap passive materials or by QD size tunability. This gives it a great interest due to their applications in many areas ranging from optical communications to biotechnology [2]. While III-V semiconductor QDs are cover the infrared spectral region, the wide gap II-VI combinations emit in the visible region where our eye sensitivity is by far the highest [3].

CdSe QDs (II-VI semiconductors) attracts a great importance due to their high luminescence efficiency (quantum yield ~50% in the visible range). This makes them a good candidates as active media for single photon emitters [4]. Their emission wavelength can be tuned from red to blue (640-480 nm). The strong interest in CdSe QDs is mainly based on the possible applications in light emitting devices in the yellow, blue, and green spectral region. CdSe semiconductor QDs can be used in many physical, chemical and medical applications by special design and a custom known as a core/shell structure where CdSe core is used with higher bandgap material like ZnSe where there are a small lattice mismatch between them (around 7%) [5].

CdSe core/shell structure is used in both chemical, biotechnology and photonic applications. For example, they used as intracellular pH sensors since their photoluminescence have pH-dependence [2]. In photonics, there are also applications, where the demand for increased data transmission and processing capacity requires creating a new generation of devices for photonic ultrahigh density integrated circuits, the core-shell structure is also proposed for nanophotonic waveguide [6].

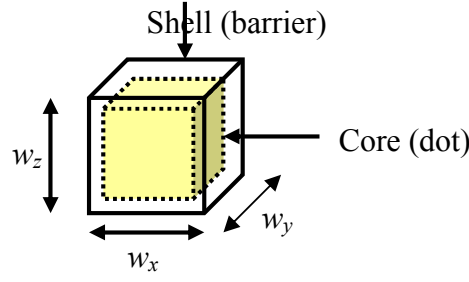
Accordingly, we study here the use of CdSe/ZnSe in a core/shell structure calculating the energy levels assuming parabolic bands then, emission, absorption and their possibility to use as optical amplifiers from the point of its characteristics in amplification and noise characteristics are studied.

2. Gain of QDs

Assuming that the QD SOA studied have a QD structures in the form of a quantum boxes, see Figure 1, with box dimensions w_x , w_y and w_z . To calculate gain we need to specify quasi-Fermi energies E_{fc} and E_{fv} , which are specified from the carrier densities for electrons N and holes P in the QD active region, assuming that ($P \approx N$), they are given by [6].

$$N = \sum_{nml} \frac{2}{\left[1 + \exp\left(\frac{E_{cnml} - E_{fc}}{kT}\right) \right]} w_x w_y w_z = \sum_{nml} \frac{2 \cdot f_c(E_{cnml})}{w_x w_y w_z} \quad (1)$$

$$P = \sum_{nml} \frac{2}{\left[1 + \exp\left(\frac{E_{fv} - E_{vnml}}{kT}\right) \right]} w_x w_y w_z = \sum_{nml} \frac{2 \cdot (1 - f_v(E_{vnml}))}{w_x w_y w_z} \quad (2)$$

Figure 1. Diagram of core/shell quantum box.

Where E_{cnml} and E_{vnml} are the allowed QD electron and hole energies, respectively, f_c and f_v are the corresponding Fermi distribution functions for electrons in the conduction and valence bands, respectively. The factor of two takes into account the electron spin states per level. The summation runs over all the confined energy states, which depends on the QD material and the core/shell conduction and valence band offsets that enable electron and hole confinement. Calculating E_{fc} and E_{fv} as specified above, one can obtain the linear absorption, $\alpha(w)$, and emission, $e(w)$, coefficients in the QD which are defined by [6]

$$\alpha(w) = \frac{w}{n_r} \sqrt{\frac{\mu_o}{\epsilon_o}} \sum_{nml} \int_{E_g}^{\infty} \langle R_{cv}^2 \rangle \times \frac{g_{cv} f_v(E_1) [1 - f_c(E_2)] \left(\frac{\hbar}{\tau_{in}}\right)}{(E_{cv} - \hbar w)^2 + \left(\frac{\hbar}{\tau_{in}}\right)^2} dE_{cv} \quad (3)$$

$$e(w) = \frac{w}{n_r} \sqrt{\frac{\mu_o}{\epsilon_o}} \sum_{nml} \int_{E_g}^{\infty} \langle R_{cv}^2 \rangle \times \frac{g_{cv} f_c(E_2) [1 - f_v(E_1)] \left(\frac{\hbar}{\tau_{in}}\right)}{(E_{cv} - \hbar w)^2 + \left(\frac{\hbar}{\tau_{in}}\right)^2} dE_{cv} \quad (4)$$

Where R_{cv} is the dipole moment, n_r is the refractive index and g_{cv} is the QD density of states given as [6]

$$g_{cv} = \frac{2\delta(E_{cv} - E_{cnml} - E_{vnml} - E_g)}{w_x w_y w_z} \quad (5)$$

Where τ_{in} is the intraband relaxation time. Eqs. (3) and (4) specify the rates of absorption and emission per unit length chosen with E_1 and E_2 as the hole and electron energy levels in the conduction and valence band energy levels, respectively. The net gain of the system is then given by

$$G(w) = e(w) - \alpha(w) \quad (6)$$

3. QD-SOA Characteristics

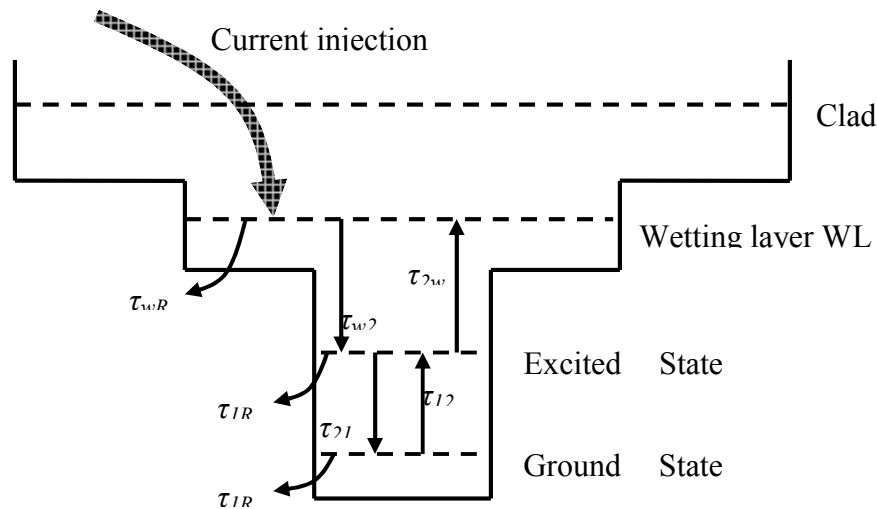
The carrier emission, recombination and relaxation between the two-dimensional wetting layer and the QD states, defined here by the QD ground state (GS) and excited state (ES), in the QD structure are described by the rate equations (REs) system. Note that, the hole dynamics are neglected due to their larger effective mass [7]. The energy diagram describing the REs system is shown in Figure 2. Accordingly the rates of the WL carrier density (N_w), ES occupation probability (h) and GS occupation probability (f) can be described by the following REs system [7],

$$\frac{\partial N_w}{\partial t} = \frac{J}{qL_w} - \frac{N_w(1-h)}{\tau_{w2}} + \frac{N_w h}{\tau_{2w}} - \frac{N_w}{\tau_{wR}} \quad (7)$$

$$\frac{\partial h}{\partial t} = \frac{N_w L_w (1-h)}{N_Q \tau_{w2}} - \frac{N_w L_w h}{N_Q \tau_{2w}} - \frac{(1-f)h}{\tau_{21}} + \frac{f(1-h)}{\tau_{12}} \quad (8)$$

$$\frac{\partial f}{\partial t} = \frac{(1-f)h}{\tau_{21}} - \frac{f(1-h)}{\tau_{12}} - \frac{f^2}{\tau_{1R}} - \frac{g_p L}{N_Q} (2f-1) S_{av} \frac{c}{\sqrt{\epsilon_s}} \Gamma \quad (9)$$

Figure 2. Energy diagram of the QD-SOA system.



where J is the current density, q is the electron charge L_w is the effective thickness of the active layer, τ_{w2} is the carrier relaxation time from WL to the ES, τ_{2w} is the carrier escape time from the ES to the WL, τ_{1R} and τ_{wR} are the spontaneous recombination times in QDs and in the WL, respectively, τ_{21} is the carrier relaxation time from the ES to GS, τ_{12} is the carrier escape time from the GS to the ES, N_Q is the surface density of QDs, ϵ_s is the dielectric constant, and Γ is the optical confinement factor. According to Pauli's exclusion principle, the occupation probability in the QD GS is given as $f = N/2(N_Q/w_x)$ [8] where N is the QD carrier density. The average signal photon density S_{av} is given by [9],

$$S_{av} = \left[\frac{(G_{FP} - 1)(1 - R_f)(1 + R_b G_{FP})}{(1 - \sqrt{R_f R_b} G_{FP})^2 + 4\sqrt{R_f R_b} G \sin^2 \Phi} \right] \frac{P_{in} n_g}{\hbar \omega_p L_w D L g_p c} \quad (10)$$

Note that; P_{in} is the input signal power, n_g is the group refractive index, \hbar is the normalized Plank's constant, ω_p is the peak frequency, D is the width of the active layer, L is the cavity length, g_p is the peak material gain, c is the free space light speed. The Fibry-Perot amplifier gain G_{FP} is given by [9],

$$G_{FP} = \frac{(1 - R_f)(1 - R_b)G_s}{(1 - \sqrt{R_f R_b} G_s)^2 + 4\sqrt{R_f R_b} G_s \sin^2 \Phi} \quad (11)$$

R_f is the front mirror reflectivity, R_b is the back mirror reflectivity. Φ is the phase angle while G_s is the single-pass gain of the SOA structure, given by [9]

$$G_s = \exp\left[(g_p \Gamma - \alpha_{int})L\right] \quad (12)$$

where α_{int} is the loss coefficient.

Rate Equations model (Eqs. 8-10) are solved at steady state case using the expression of the average signal photon density S_{av} , Eq. (11). The noise added to the signal during the amplification process is a fundamental property for every kind of amplifiers. The noise characteristics of an amplifier are quantified by a parameter called noise figure. The noise in semiconductor devices can be originates from the noise arises from spontaneous emission and (intensity and phase noise) and that results from discrete nature of carrier generation and recombination processes (shot noise). The last part is neglected in some works. [10,11]. When the shot noise part is taken into account, the amplifier noise figure can be written as [2,8]

$$F_n = 2n_{sp}(G_{FP} - 1)/G_{FP} + (1/G_{FP}) \quad (13)$$

The parameter n_{sp} is the spontaneous emission factor given by [13]

$$n_{sp} = \frac{\Gamma e(w)}{[\Gamma G(w)] - \alpha_{int}} \quad (14)$$

$G(w)$ is the net gain as defined in Eq. (6) and $e(w)$ is linear emission coefficient as defined in Eq. (4).

4. Results and Discussion

Typical values of the material parameters are listed in Table 1 for CdSe/ZnSe system. In addition, we use ($E_g = 1.7$ eV, $m_e = 0.144m_o$ and $m_v = 0.453m_o$) for CdSe and ($E_g = 2.8$ eV, $m_e = 0.122m_o$ and $m_v = 0.504m_o$) for ZnSe [8].

Table 1. Parameters used in the Calculations [5]

Parameter	Value	Unit
L	200	μm
L_w	0.2	μm
D	10	μm
N_Q	5×10^{10}	cm^{-2}
τ_{in}	0.1	ps
τ_{w2}	3	ps
τ_{2w}	1	ns
τ_{12}	1.2	ps
τ_{21}	0.16	ps
τ_{1R}	0.4	ns
τ_{wR}	1	ns
Φ	0	
$R_f = R_b$	10^{-4}	
α_{int}	3	1/cm
Γ	0.006	
L_b	20	nm
L_c	75	nm
P_{in}	1	μW

We, first, calculate energy conduction and valence bands by using the quantum box model. Note that, the quantum box dimensions are assumed to be $w_x = w_y = w_z = 10\text{nm}$. The calculated subbands are used to calculate linear absorption and emission coefficients. The structure used in the calculations constructed from the active layer (QD + barrier (20 nm)) surround by clad layer (75 nm). we calculate structures with one layer and six layers (see Fig. 2). Gain coefficients is calculated using Eq. (7). All calculations are done at carrier density $2 \times 10^{24} \text{m}^{-3}$ unless states otherwise.

Figure 3 shows the linear absorption and emission coefficient versus wavelength. The emission coefficient higher than the absorption coefficient by >6 times. Note here, the peak wavelength ~ 697 nm which is in the range of measurements in [7]. The result of emission and absorption can be compared with that in [6]. The emission (and absorption) values are higher than that obtained for InGaAs/InP QD cubes while the peak wavelength here lies between wavelengths of InGaAs/InP and CdSe/ZnS.

Figure 3. Linear absorption and emission coefficients.

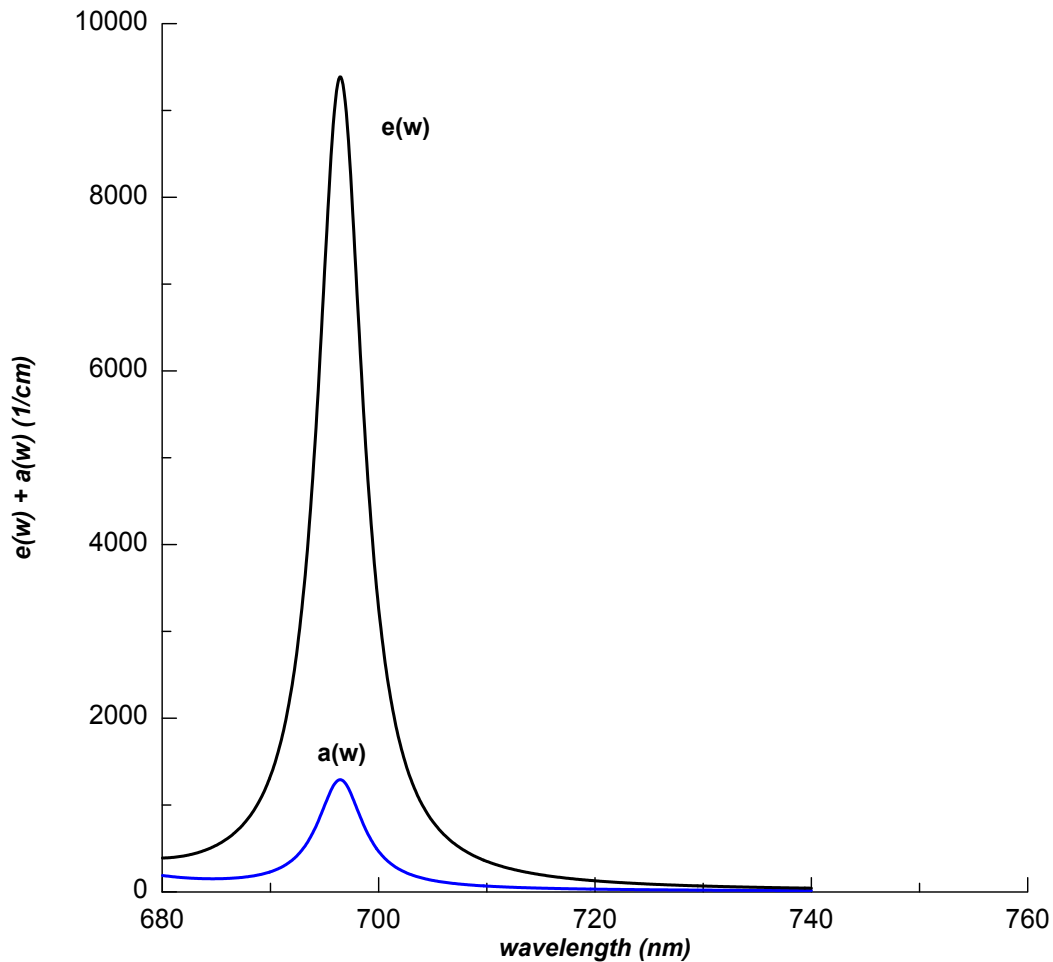


Figure 4 (a) shows the small signal gain variation with increasing the number of active layers where approximately 28dB gain at six layers is obtained at 400 mA. For InAs QDs, ~ 25 dB gain is obtained for 3 layers at 200 mA [12], while ~ 18 dB gain is obtained for InGaAs/GaAs QDs with 15 layers [9]. The relation between small-signal gain and current is shown in figure 4 (b). One can compare the results here with that in [14] where a 15 dB gain is obtained for InAs/InP QDs for 40 mA emits at 1550 nm. Here, approximately, the same gain is obtained at this current.

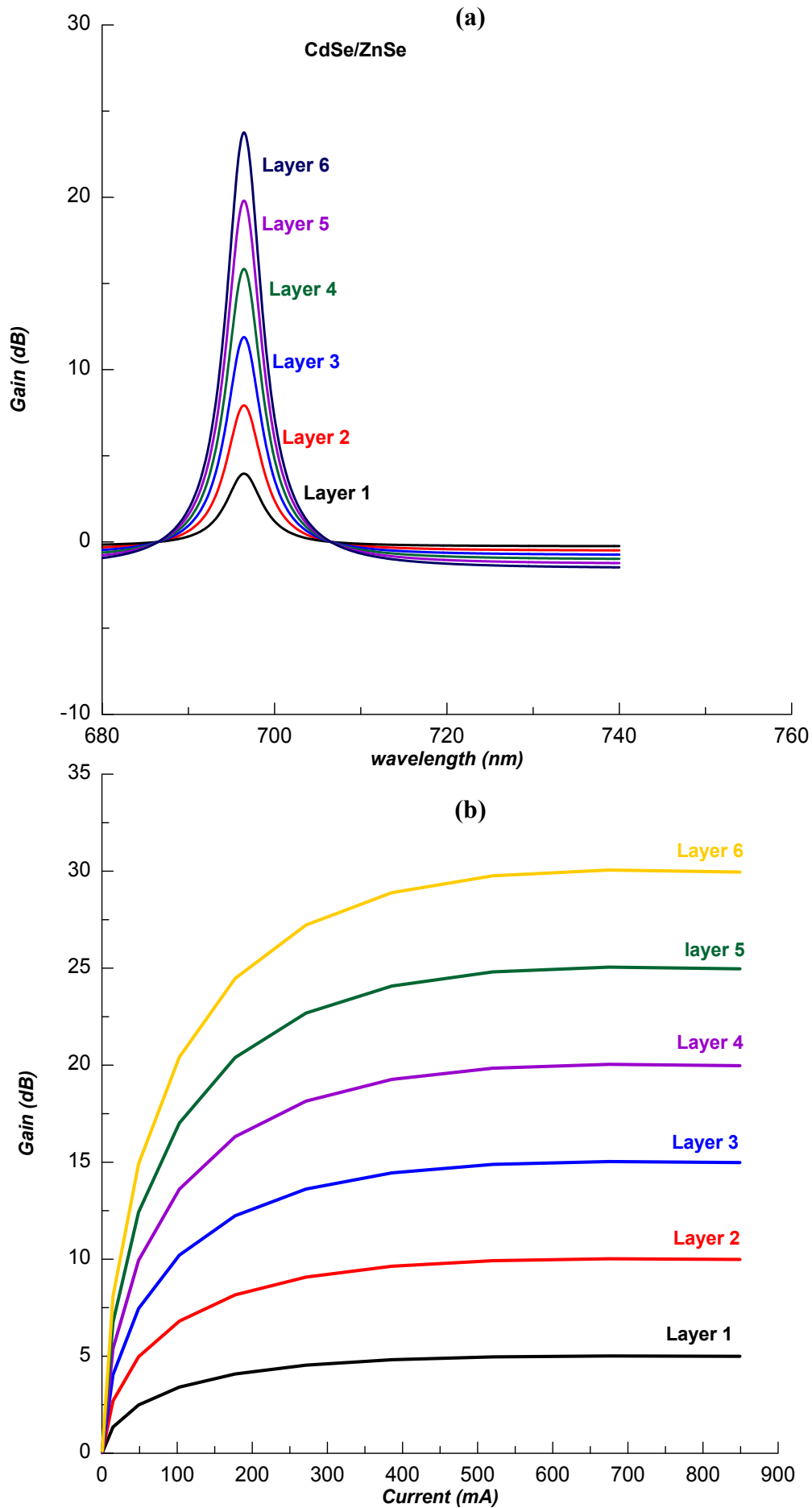
Figure 4. Small-signal gain versus (a) wavelength (b) current, for different active layers.

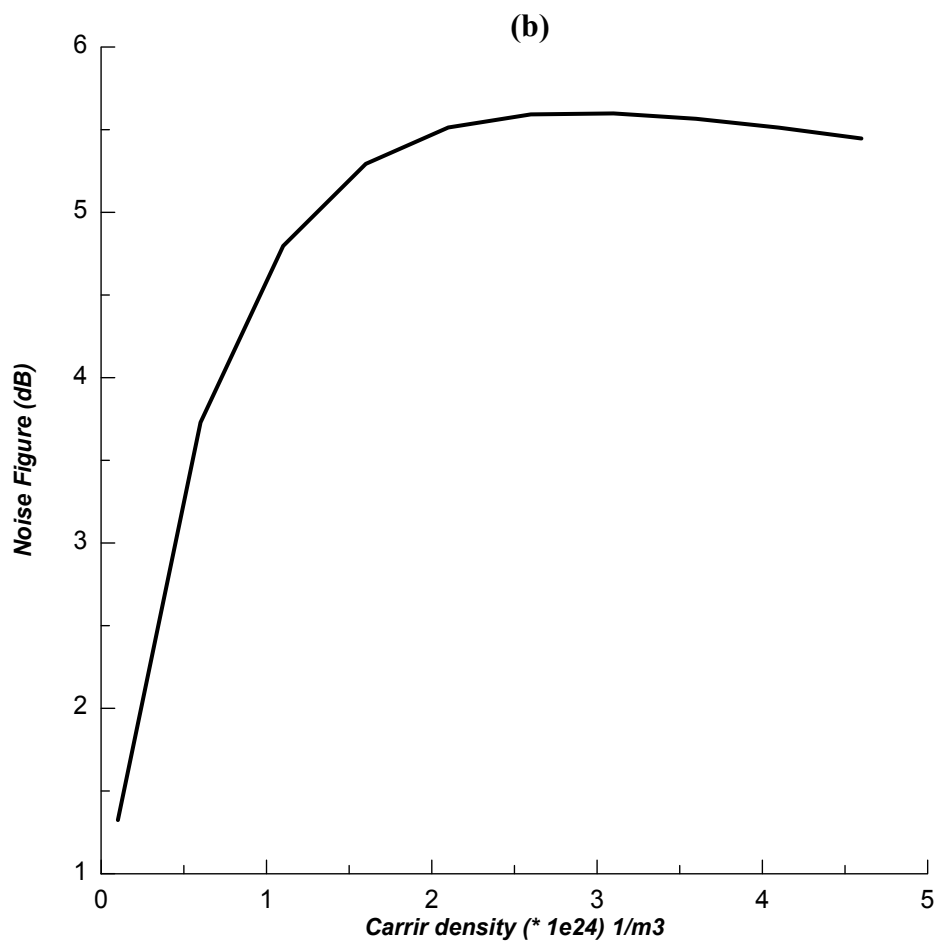
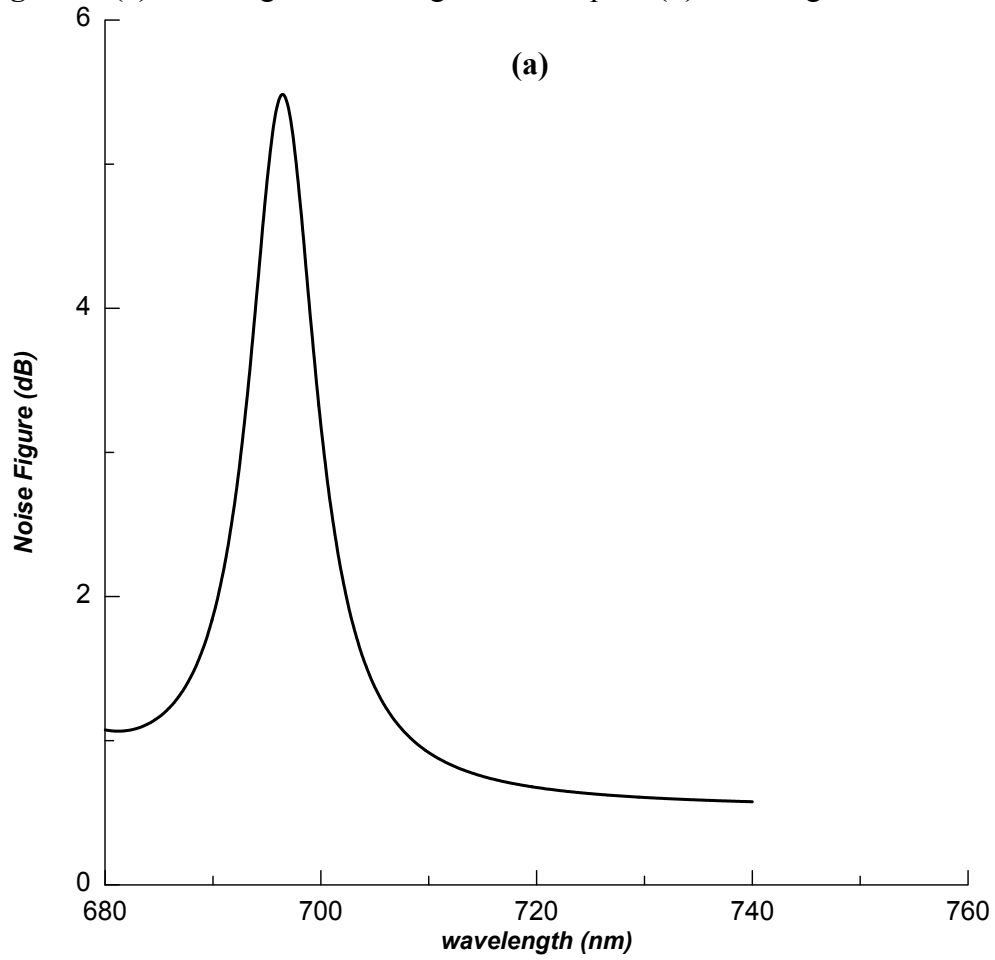
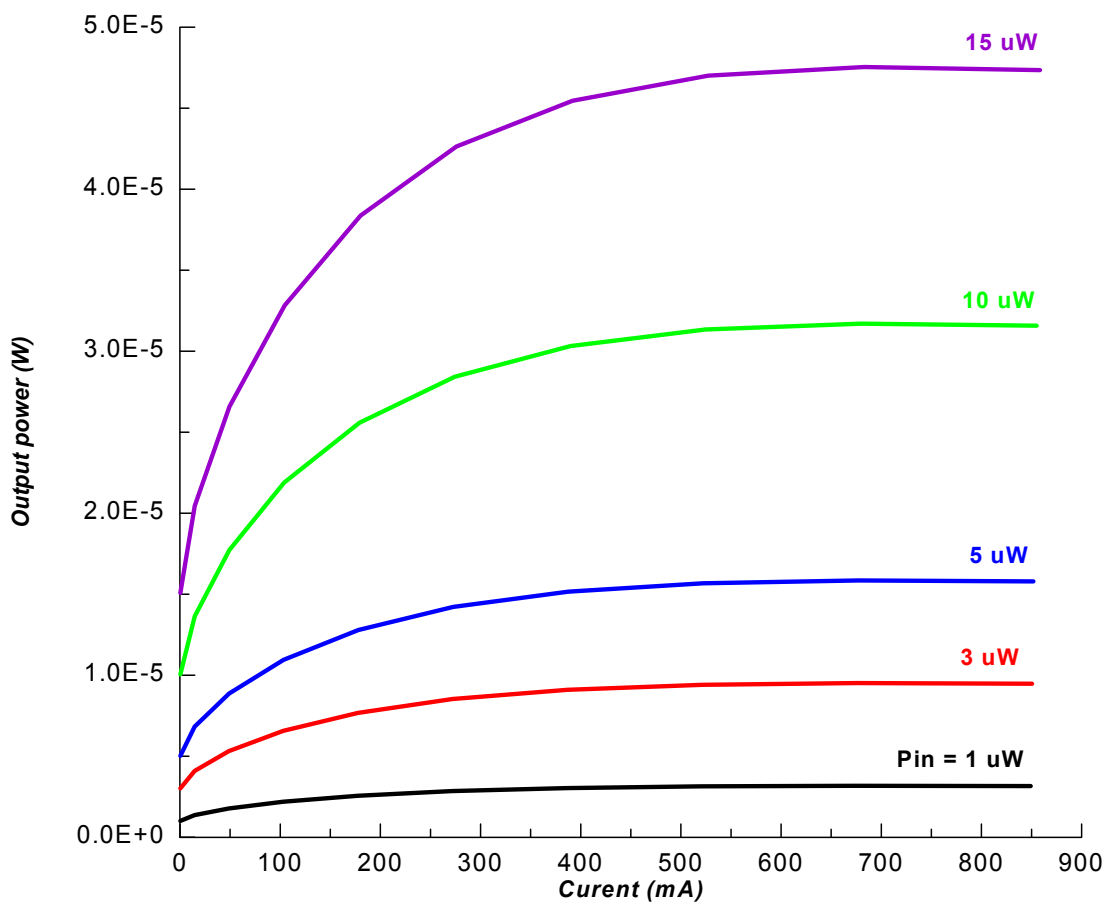
Figure 5. (a) Noise figure including shot noise part. **(b)** Noise figure-current relation.

Figure 5 (a) shows the noise figure for CdSe/ZnSe QD-SOA, where a low noise can be obtained for these structures. Figure 5 (b) shows the relation between noise figure and current. Figure 6. show the output power obtained from CdSe/ZnSe QD-SOAs versus current at input powers (1, 3, 5, 10, 15 μW). At 100mA injection current, a $30\mu\text{W}$ output power can be obtained. At 600mA, a $45 \mu\text{W}$ output power can be obtained.

A QD core/shell structure can be used to built nanophotonic integrated circuit. This structure is a QD waveguide where the signals are propagated in forward and backward directions then, they amplified after traversing the structure. This structure can be represented as basis unit of the building block of the nanophotonic devices. So, the simulated structure can be used to develop photonic integrated circuits.

Figure 6. Output power versus current at different values of input power.



4. Conclusion

CdSe/ZnSe QD SOA is simulated. The core/shell structure is assumed. The QDs are assumed to be in the form of quantum boxes with 10nm box dimension. The emission, absorption and noise figure are studied. The results show that the structure have a high small-signal gain, compared with other structures, and a low noise figure which permit to use it to built a nanophotonic circuits.

References

- [1] Mansoori GA. Principles of Nanotechnology (Molecular-Based Study of Condensed Matter in Small Systems), World Sci Pub Co, **2005**.
- [2] Liu Y-S, Sun Y, Vernier PT, Liang C-H, Chong SYC et al. pH-sensitive Photoluminescence of CdSe/ZnSe/ZnS Quantum Dots in Human Ovarian Cancer Cells. *J Phys Chem C Nanomater Interfaces* **2007**; 111(7): 2872–2878.
- [3] Hommel D, Leonardi K, Heinke H, Selke H, Ohkawa K, Gindele F, Woggon U. CdSe/ZnSe Quantum Dot Structures: Structural and Optical Investigations. *Phys. Stat. Sol. (b)* **1997**; 202, 835-43
- [4] Chen H, Hsu C, Hong H. InGaN–CdSe–ZnSe quantum dots white LEDs. *IEEE Phot. Tech. Lett.* **2006**; 18(1): 193-195.
- [5] Schmidt Th, Clausen T, Falta J, Alexe G, Passow T, Hommel D, Bernstorff S. Correlated stacks of CdSe/ZnS quantum dots. *Appl. Phys. Lett.* **2004**; 84 (22): 4367-69.
- [6] Wang C-J, Lin LY, Parviz BA. Modeling and simulation for a nano-photonic quantum dot waveguide fabricated by DNA-directed self-assembly. *IEEE J. of Selected Topics in Quantum Electronics* **2005**; 11(2): 500-509.
- [7] Ben-Ezra Y, Haridim M, Lembrikov B-I. Theoretical analysis of gain-recovery time and chirp in QD-SOA. *IEEE J. Quantum Electronics* **2005**; 17(9): 1803-1805.
- [8] M. A. Al-Mossawi, A. H. Al-Khursan, R. A. Al-Ansari, “ZnO-MgZnO Quantum-Dot Semiconductor Optical Amplifiers” *Recent Patents on Electrical Engineering* **2009**; 2: 226-238.
- [9] M. Vasileiadis, D. Alexandropoulos, M. J. Adams, H. Simos and D. Syvridis, “Potential of InGaAs/GaAs Quantum Dots for Applications in Vertical Cavity Semiconductor Optical Amplifiers” *IEEE J. of Selected Topics in Quantum Electronics* **2008**; 14(4): 1180-1187.
- [10] Agrawal G-P, Dutta N-K. Long Wavelength Semiconductor Lasers. Van Nostrand Reinhold, New York, 1986.
- [11] Al-Khursan A-H. Intensity noise characteristics in Quantum-Dot Lasers: Four-Level Rate Equations Analysis. *J Luminescence* **2005**; 113(1-2): 129-36.
- [12] Xiao J-L, Huang Y-Z. Numerical Analysis of Gain Saturation, Noise Figure, and Carrier Distribution for Quantum-Dot Semiconductor-Optical Amplifiers. *IEEE J. Quantum Electronics* **2008**; 44 (5): 448-455.
- [13] Forestieri E. Optical Communication Theory and Techniques Ch. 8, Springer, Pisa, Italy, **2005**.
- [14] Ben-Ezra Y, Lembrikov B-I, Haridim M. Acceleration of gain recovery and dynamics of electrons in QD-SOA. *IEEE J. Quantum Electronics* **2005**; 41(10): 1268-1273.

© 2012 by the authors; licensee Insciences Journal.

Open Access article under the terms and conditions of Creative Commons Attribution Non-Commercial License 3.0 Unported.